



HAL
open science

Atmospheric Plasma Deposition: A new pathway in the design of Conducting Polymer-based Anodes for Hydrogen Fuel Cells

Marc Michel, Jérôme Bour, Julien Petersen, Claire Arnoult, Frank Eттingshausen, Christina Roth, David Ruch

► **To cite this version:**

Marc Michel, Jérôme Bour, Julien Petersen, Claire Arnoult, Frank Eттingshausen, et al.. Atmospheric Plasma Deposition: A new pathway in the design of Conducting Polymer-based Anodes for Hydrogen Fuel Cells. *Fuel Cells*, 2010, 10 (6), pp.932. 10.1002/fuce.201000050 . hal-00574812

HAL Id: hal-00574812

<https://hal.science/hal-00574812>

Submitted on 9 Mar 2011

HAL is a multi-disciplinary open access archive for the deposit and dissemination of scientific research documents, whether they are published or not. The documents may come from teaching and research institutions in France or abroad, or from public or private research centers.

L'archive ouverte pluridisciplinaire **HAL**, est destinée au dépôt et à la diffusion de documents scientifiques de niveau recherche, publiés ou non, émanant des établissements d'enseignement et de recherche français ou étrangers, des laboratoires publics ou privés.



Atmospheric Plasma Deposition: A new pathway in the design of Conducting Polymer-based Anodes for Hydrogen Fuel Cells



Journal:	<i>Fuel Cells</i>
Manuscript ID:	fuce.201000050.R1
Wiley - Manuscript type:	Original Research Paper
Date Submitted by the Author:	24-May-2010
Complete List of Authors:	Michel, Marc; Centre de Recherche Public Henri Tudor, Advanced Materials and Structures Bour, Jérôme; Centre de Recherche Public Henri Tudor, Advanced Materials and Structures Petersen, Julien; Centre de Recherche Public Henri Tudor, Advanced Materials and Structures Arnoult, Claire; Centre de Recherche Public Henri Tudor, Advanced Materials and Structures Ettingshausen, Frank; TU Darmstadt, Institute for Materials Science Roth, Christina; TU Darmstadt, Institute for Materials Science Ruch, David; Centre de Recherche Public Henri Tudor, Advanced Materials and Structures
Keywords:	Fuel Cell Electrode, Plasma Deposition Technology, MEA Preparation, Fuel Cell Technology, Assemblies



Atmospheric Plasma Deposition: A new pathway in the design of Conducting Polymer-based Anodes for Hydrogen Fuel Cells

Marc Michel¹, Jérôme Bour¹, Julien Petersen¹, Claire Arnoult¹, Frank Ettingshausen²,
Christina Roth² and David Ruch¹

¹*Centre de Recherche Public Henri Tudor, Department of Advanced Materials and
Structures, Esch-sur-Alzette, L-4002, Luxembourg*

²*Institute for Materials Science, TU Darmstadt, D-64287 Darmstadt, Germany*

Abstract

In this study, we explored thin films of nanofibrous functionalized conducting plasma Polyaniline (pPANI) with platinum deposited by an atmospheric plasma deposition process for the potential design of anodes for hydrogen fuel cell applications. We observed that the incorporation of such a polymer, characterized by both electronic and ionic conductivity, associated with a catalyst in a 3D porous network, could lead to an increased probability of the three-phase contact to occur. In this context, aniline was mixed with functionalized platinum nanoparticles and used as the precursor. The role of these functionalized nanoparticles was not only to act as the catalyst for fuel cell purposes, but also as nucleation sites promoting the formation of the nanofibrous pPANI thin film during the plasma polymerization. The morphology of the thin film was analyzed by scanning electron microscopy and the efficiency, in terms of energy conversion, was assessed in a single fuel cell test bench.

Introduction

Polymer electrolyte membrane fuel cells (PEMFC) are being considered as promising candidates for a number of commercial applications including their use in portable electronic devices and automobiles. One of the key challenges facing the widespread commercialization of PEM fuel cells is their high cost. The cost is largely associated with expensive materials such as a noble metal catalyst, and inefficiencies in their utilization due to a weak control on the so called triple phase boundary (TPB) [1], which is located in the membrane electrode assembly (MEA). To effectively utilize the catalyst, these regions, corresponding to the interfacial areas between the reactant, electrolyte and catalyst, must balance the ionic and electronic conducting media, allowing continuous pathways of the protons to the electrolyte and electrons to the electrode. These media influence the hydrophilic and hydrophobic properties of the composite material bringing a design challenge at the nanometer scale due the necessary integration of disparate materials.

In this context, it has been shown elsewhere that electrodes fabricated by incorporating a polymer, characterized by both ionic and electronic conductivity, in a so called Layer-by-Layer (LbL)[2] architecture can give a significant boost to the fuel cell performance, whereas less catalyst is employed. [3-10] Despite very promising results, this method of preparation can only be done in a batch process.

Inspired by these works, this paper aims at designing a new generation of multilayered anodes using Atmospheric Plasma Polymerization, which has become a promising technology for in-line processing. Plasma polymerization is a versatile technique for the deposition of plasma polymer films with functional properties suitable for a wide range of applications such as protective coatings, biomedical materials, electronic and optical devices or adhesion promoters. [11-13] For example, plasma-induced polymerization has been extensively used for the preparation of conducting polymeric thin films including polyaniline (PANI). In

1
2
3 particular, Tiwari et al. have shown that nanofibers of conducting polyaniline (PANI) thin
4
5 film can be obtained and they explored its application in the fabrication of NO₂ gas sensor.
6
7 [14]
8
9

10 It is now well-established that plasma polymers are different from those fabricated by
11
12 conventional wet synthetic methods: they are usually branched, highly cross-linked, insoluble,
13
14 pinhole-free, and adhere well to most substrates.
15

16
17 Nevertheless, plasma-polymerization is mostly performed at low pressure, limiting its
18
19 application to batch processes. In addition, low pressure plasma technology requires the use of
20
21 costly vacuum pumping systems. [15]
22
23

24 Among various atmospheric pressure plasmas, dielectric barrier discharges (DBDs) [16] have
25
26 received a lot of attention due to the easy formation of a stable discharge and their scalability.
27
28 These discharges are usually generated in the space between two parallel electrodes, at least
29
30 one of these being covered with a dielectric layer. [17-18]
31
32

33 The functionality of the plasma deposited layer is mainly determined by the nature of the used
34
35 vapour precursors or monomers. [19] These precursors or monomers, which lead to the
36
37 coating formation, are diluted in a carrier gas, which is usually helium, argon, or nitrogen.
38
39

40 In this study, we explored nanofibrous pPANI thin films deposited using the atmospheric
41
42 pressure dielectric barrier discharge process for the design of potential anodes for hydrogen
43
44 fuel cell applications. We expect that the incorporation of such a polymer, characterized with
45
46 electronic and ionic conductivity and associated with a catalyst in a 3D porous network could
47
48 lead to an increased probability of the three-phase contact to occur. In this background aniline
49
50 was mixed with functionalized platinum nanoparticles and used as the precursor. The role of
51
52 these functionalized nanoparticles was not only to act as a catalyst for fuel cell purposes, but
53
54 also as nucleation sites promoting the formation of the nanofibrous pPANI thin film during
55
56 the plasma polymerization. The morphology of the thin film was analyzed by scanning
57
58
59
60

1
2
3 electron microscopy and the efficiency, in terms of energy conversion, was evaluated in a
4 commercial single fuel cell test bench.
5
6

7
8 To our knowledge, this paper is the first showing that electrodes for fuel cells can be
9 manufactured by a sequential atmospheric pressure dielectric barrier discharge process of
10 aniline and functionalized platinum.
11
12
13
14
15
16

17 **Experimental section**

18 **Materials**

19
20 Hexylamine, sodium borohydride (NaBH_4) 99%, 4-Aminothiophenol (mercaptoaniline),
21 Aniline, and platinum (IV) chloride (PtCl_4) 99.99% were obtained from Aldrich and used as
22 received. PtCl_4 was stored in a dessicator under vacuum.
23
24
25
26
27
28

29 **Functionalization of Platinum nanoparticles**

30
31 The synthesis and the functionalization of platinum nanoparticles were strongly inspired by a
32 previous work. [20] Briefly, 150 mg PtCl_4 was dissolved in 35 mL of hexylamine in a 200 mL
33 flask leading to the formation of an orange solution (solution 1). Then, 165 mg of 4-
34 Aminothiophenol was dissolved in 15 mL of a methanol/hexylamine solution (50/50)
35 (solution 2). Finally, 150 mg of NaBH_4 was dissolved in 20 mL of a water/methanol solution
36 (50/50). 10 mL of hexylamine was added after complete dissolution of sodium borohydride
37 (solution 3). Solution 3 was then poured into solution 1 under vigorous stirring at room
38 temperature. The reaction mixture turned brown within a few seconds. After 30 s, solution 2
39 was added to the mixture. After 5 min, 100 mL of Milli-Q water was added. The resulting
40 solution was then stirred for 20 min before being transferred into a separatory funnel. Just
41 after phase separation, the water was removed and the organic phase was repeatedly washed
42 with the same amount of water (100 mL). The volume of the dark brown organic phase was
43 reduced to ca. 1-2 mL by rotary evaporation at 30 °C and transferred into a centrifuge tube
44
45
46
47
48
49
50
51
52
53
54
55
56
57
58
59
60

1
2
3 with 0.1 g of 4-Aminothiophenol dissolved in 7.5 mL of ethanol. After this solution was
4
5 stirred overnight, a black solid residue was recovered by centrifugation. The supernatant
6
7 presumably contained unreacted 4-Aminothiophenol and platinum complexes. The precipitate
8
9 was washed with pure ethanol and centrifuged again. The fraction yielded to a dark brown
10
11 solution, which remained stable for several weeks.
12
13
14
15
16

17 **Plasma polymerization**

18
19 In this study, the precursor used for the plasma polymerization consisted of 5 mL of
20
21 functionalized platinum solution mixed with 5 mL of aniline (adjusted at pH=2).
22
23

24
25 The DBD discharge was generated between an earthed bottom aluminium plate and two high-
26
27 voltage aluminium top plates protected by a 3.25-mm-thick glass plate. The gap between the
28
29 electrodes was set to 2 mm.
30

31
32 A commercial Nafion 117 membrane was used as the substrate and was positioned at the
33
34 bottom electrode. The precursor was atomized by a TSI 3076 system at a constant atomization
35
36 pressure of $2 \cdot 10^5$ Pa and injected into the gas before entering the plasma zone. The carrier gas
37
38 composition, which was set by mass flow controllers, consisted of a N_2/O_2 (97/3 vol. %)
39
40 mixture with a gas flow of $20 \text{ L} \cdot \text{min}^{-1}$. The gas mixture containing the precursor aerosol was
41
42 injected into the plasma through a slit between the two top electrodes. The experiment was
43
44 carried out at atmospheric pressure and at room temperature. During the experiment, the top
45
46 electrode block moved over the sample at a constant speed ($4 \text{ m} \cdot \text{min}^{-1}$) and in a range of 380
47
48 mm. The plasma coating consisted of 100 passes and lasted 10 min leading to the formation
49
50 of a greenish film on the Nafion 117 membrane. For the coating process, plasma discharges
51
52 were generated by an AC power supply with variable frequency. The frequency was set to 1.5
53
54 kHz and the voltage was a pseudo sinusoid as a function of time. Power was kept constant
55
56
57
58
59
60

1
2
3 during the experiment and was set to 500 W, which corresponded to a power density (over the
4 electrodes) close to 0.8 W.cm⁻².
5
6
7
8
9

10 **Characterization Techniques**

11 **Materials characterization**

12
13 The chemical structure of the coatings was evaluated by FTIR spectroscopy using a Bruker
14 Optics Tensor 27 spectrometer. UV-Visible investigations were obtained by using a Perkin
15 Elmer lambda 35 Spectrophotometer.
16
17
18
19
20
21

22 The pPANI-Pt fibers were investigated by X-ray powder diffraction using a diffractometer
23 STOE STADI-P with Germanium monochromated Cu_{Kα} radiation ($\lambda = 1.54060 \text{ \AA}$) and a
24 position-sensitive detector with 40° aperture. Average particle sizes are estimated by the
25 Scherrer equation.
26
27
28
29
30
31

32 In addition, transmission electron microscopy (TEM) was employed to measure the Pt particle
33 size and the particle distribution. A JEOL 3010 high resolution electron microscope equipped
34 with LaB₆ filament and an acceleration voltage of 300 kV was used for the measurements. A
35 small amount of the platinum dispersion was placed on a holey-carbon film covered Cu grid
36 and left to evaporate.
37
38
39
40
41
42

43 The platinum loading on the pPANI was obtained by thermogravimetric analysis (TGA) with
44 a Netzsch STA 490 under synthetic air (Linde(R), 80% N₂, 20% O₂) atmosphere from 30 to
45 1000 °C with a heating rate of 5 °C min⁻¹.
46
47
48
49
50

51 The morphology of the LBL films was checked by scanning electron microscopy (SEM)
52 using a JEOL JSM 6340 field-emission gun scanning electron microscope. The MEA was cut
53 into tiny pieces and deposited onto a SEM holder before being observed.
54
55
56
57
58
59
60

Fuel cell testing

The MEA was tested in a single cell fuel cell test bench using a commercial cell hardware (Electrochem. Inc.) and was conditioned over night, until a steady state current was reached at a potential of 0.6 V. In hydrogen operation, 150 ml min⁻¹ H₂ (N 5.0, Linde) are loaded with water in a humidifier (T=70 °C) and fed into the fuel cell anode. As cathode feed, high-purity oxygen was supplied (N 4.5, Linde) at 75 ml min⁻¹ to the fuel cell pre-heated to 80 °C. Current–voltage curves were obtained galvanostatically using an operated fuel cell test bench.

Results and discussion

Functionalization and characterization of Platinum nanoparticles

A major point for the design of the MEA by plasma polymerization was the control of the particles size after their functionalization with mercaptoaniline. It was expected in this work that the use of a mixture of aniline and functionalized platinum particles could help to promote the formation of aniline plasma polymer thanks to nucleation processes occurring during the coating. This functionalization was based on the reduction of platinum salt by a reducing agent (NaBH₄) in the presence of mercaptoaniline. [20] The synthesis described here used hexylamine as the intermediate capping agent. The final capping agent was introduced in the reaction mixture directly after reduction of the platinum salt. The rapid addition of mercaptoaniline after platinum reduction was consequently required in order to avoid irreversible particle flocculation phenomena.

Infrared spectroscopy was performed on the functionalized nanoparticles solution in order to check the presence of mercaptoaniline surrounding platinum nanoparticles (Figure 1).

Absorption peaks above 3000 cm⁻¹ are attributed to N-H stretching modes whereas the peak located at 1612 cm⁻¹ is characteristic of NH₂ deformation. The C-N stretching mode is located at 1272 cm⁻¹. The aromatic ring exhibits vibrations at 1578 and 1480 cm⁻¹ corresponding to

1
2
3 aromatic ring stretching modes. Absorption corresponding to C-H bonds appears at 1172 cm^{-1}
4
5 (in-plane bending modes) and 815 cm^{-1} (C-H wagging vibration).
6
7

8 The morphology of the functionalized platinum was investigated by TEM. On the TEM
9
10 pictures (Figure 2), one can see the presence of individual particles, suggesting that the
11
12 functionalization had a positive effect on the dispersion: no aggregation was observed. The
13
14 good dispersion can be explained by the fact that the presence of mercaptoaniline acted as a
15
16 powerful capping agent. Note that this dispersion was kept stable for several months. The
17
18 particles ranged in size from 1 to 4.5 nm with a maximum centred around 3 nm (Figure 3).
19
20
21
22
23

24 **Manufacturing of a fuel cell anode using plasma polymerization**

25
26 The underlying idea was to use the functionalized nanoparticles as nucleation agent able to
27
28 promote the formation of pPANI. The plasma polymer film was directly deposited onto a
29
30 commercial Nafion 117 membrane.
31
32

33
34 As mentioned previously, fuel cell electrodes require three essential properties: they should be
35
36 electrically conductive, proton conductive and able to trigger a chemical reaction catalyzed by
37
38 a metal. From the SEM images (Figure 4 A, B), one can see the presence of pPANI-Pt fibers
39
40 with a diameter range of 50-70 nm. The film that exhibits a total thickness of about $2.5\mu\text{m}$,
41
42 presents a strong interdigitation of pPANI fibers, suggesting a dense 3D porous network. This
43
44 morphology increases the probability of contacts between the strands, while substantial
45
46 porosity also offers efficient mass transport. Electrical conductivities were measured on the
47
48 coated film and were found to be $5 \cdot 10^{-3}\text{ S} \cdot \text{cm}^{-1}$.
49
50
51

52
53 Note that the experiment performed without Pt nanoparticles did not lead to the formation of
54
55 fibers (Figure 4 C). This point suggests that the presence of functionalized Pt nanoparticles
56
57 can act as nucleation sites, where pPANI can easily grow during the plasma process.
58
59
60

1
2
3 The amount of Pt contained in the plasma polymer films can be obtained using
4 thermogravimetric analysis (TGA) (data not shown) by completely oxidizing the fibers during
5 analysis. TGA gives a Pt loading of 16 %, which represents 0.09 mg.cm^{-2} of Pt.
6
7

8
9
10 The X-ray diffraction (XRD) patterns collected for pPANI-Pt are shown in Figure 5. The
11 diffraction peaks show that Pt nanoparticles are present in the face centered cubic (fcc)
12 structure, as indicated by the characteristic peaks of (111), (200), (220) and (311). The
13 average Pt particle size for pPANI-Pt catalysts was calculated from the broadening of the
14 (220) diffraction peak using the Scherrer equation. The calculated mean Pt particles sizes for
15 pPANI-Pt are 3.4 nm, which is consistent with the TEM observations.
16
17

18
19
20 The FTIR spectrum of the pPANI-Pt thin film is presented in Figure 6. The characteristic
21 peaks of emeraldine base form of pPANI were observed in the spectrum at 3260 cm^{-1} (N–H
22 stretching with hydrogen); 3025 cm^{-1} (aromatic C–H stretching); 1532 cm^{-1} (C–C stretching
23 of quinoid rings); 1480 cm^{-1} (C–C stretching vibration of benzenoid rings); and 1290 cm^{-1}
24 (C–N stretching). The absorption band at 1125 cm^{-1} is assigned to N–Q–N bending
25 vibration shift towards the lower wave number that corresponds to the pPANI-Pt emeraldine
26 base. This result further supports the formation of pPANI-Pt using the plasma polymerization
27 technique.
28
29

30
31
32 The pPANI-Pt thin film was characterized using a UV–visible spectrophotometer. In the
33 spectrum (Figure 7), the characteristic bands of PANI (emeraldine base) were observed at
34 310, and 513 nm, due to the π - π^* transition, polaron bands transition, and quinoid unit,
35 respectively. These absorption bands exhibit both excitations of amine nitrogen of the
36 benzenoid segments and imine nitrogen of the quinoid segments of pPANI-Pt. All these
37 features clearly indicate the formation of pPANI by the plasma polymerization.
38
39

40
41
42 The performance of the prepared membranes onto the Nafion membrane was tested in PEM
43 fuel cells (Figure 8). The film was used as anode and a standard carbon black (CB) (0.5 mg Pt
44
45
46
47
48
49
50
51
52
53
54
55
56
57
58
59
60

1
2
3 per cm^2) based catalyst was used as cathode. H_2 and O_2 are used at the anode and the cathode,
4
5 respectively. The peak power density of the whole fuel cell was as high as 80 mW cm^{-2} , the
6
7 obtained value remaining smaller than commercial fuel cells made of carbon black. This
8
9 limited performance might be due to a low value of conductivity of the pPANI film.

10
11
12 Nevertheless, the Pt utilization, which is considered as one key affecting the practical and
13
14 commercial prospects of fuel cell technology, can be obtained by dividing the peak power
15
16 density by the Pt loading. In our case, the Pt utilization was found to be as high as 880
17
18 mW/mg_{Pt} , which is a value comparable to those obtained by conventional electrode
19
20 preparation methods of electrodes. This good value can be attributed to the nanoscale 3D
21
22 organization of the plasma multilayered film adequate for balancing diverse requirements in
23
24 the electrodes, and specifically to the significantly improved accessibility of Pt particles at the
25
26 triple phase boundaries.
27
28
29
30
31
32
33

34 **Conclusion**

35
36 In this paper, we demonstrate the potential of atmospheric pressure plasma deposition for the
37
38 design of conducting polymer-based anodes for hydrogen fuel cells. This work shows that the
39
40 incorporation of functionalized platinum nanoparticles can act as nucleation sites able to
41
42 promote the formation of polyaniline fibers during the plasma process. SEM images show that
43
44 pPANI-Pt electrodes have a strong interdigitation and thus create a dense and extensive 3D
45
46 network of fibers. This particular morphology increases the probability of contacts between
47
48 the strands, while substantial porosity also offers promising mass transport. Hence,
49
50 atmospheric pressure plasma represents an interesting new pathway for creating fast and
51
52 efficient electrodes for hydrogen fuel cells.
53
54
55
56
57
58
59
60

References

- [1] R. O'Hayne, D. R. Barnett and F. F. Prinz, *J. Electrochem. Soc.*, 2005, 152, A439–A444
- [2] G. Decher, *Science*, 1997, 277, 1232–1237
- [3] T. R. Farhat and P. T. Hammond, *Abstr. Pap. Am. Chem. Soc.*, 2005, 229, U733–U734.
- [4] T. R. Farhat and P. T. Hammond, *Adv. Funct. Mater.*, 2006, 16, 433–444.
- [5] T. R. Farhat and P. T. Hammond, *Chem. Mater.*, 2006, 18, 41–49.
- [6] S. P. Jiang, Z. C. Liu and Z. Q. Tian, *Adv. Mater.*, 2006, 18, 1068–1072.
- [7] C. N. Kostelansky, J. J. Pietron, M. S. Chen, W. J. Dressick, K. E. Swider-Lyons, D. E. Ramaker, R. M. Stroud, C. A. Klug, B. S. Zelakiewicz and T. L. Schull, *J. Phys. Chem. B*, 2006, 110, 21487–21496.
- [8] M. Pan, H. L. Tang, S. P. Jiang and Z. C. Liu, *J. Electrochem. Soc.*, 2005, 152, A1081–A1088.
- [9] M. Michel, A. Taylor, R. Sekol, P. Podsiadlo, P. Ho, N. Kotov, and L. Thompson, *Adv. Mater.*, 2007, 19, 3859–3864,
- [10] M. Michel, F. Ettingshausen, F. Scheiba, A. Wolz and C. Roth, *Phys. Chem. Chem. Phys.*, 2008, 10, 3796–3801.
- [11] F. Benitez, E. Martinez, J. Esteve, *Thin Solid Films* 2000, 377–378, 109–114.
- [12] C. Vautrin-Ul, C. Boisse-Laporte, N. Benissad, A. Chausse, P. Leprince, R. Messina, *Prog. Org. Coat.* 2000, 38, 9–15.
- [13] F. Arefi, V. Andre, P. Montazer-Rahmati, J. Amouroux, *Pure Appl. Chem.* 1992, 64, 715–723.
- [14] A. Tiwari, R. Kumar, M. Prabakaran, R. R. Pandey, P. Kumari, A. Chaturvedi and A. K. Mishra, *Polym. Adv. Technol.*, 2009, DOI : 10.1002/pat.1470.

- 1
2
3 [15] R. Y. Korotkov, T. Goff, P. Ricou, Surf. Coat. Technol. 2007, 201, 7207-7215.
4
5 [16] G. Borcia, N. M. D. Brown, J. Phys. D: Appl. Phys. 2007, 40, 1927-1936.
6
7 [17] J. J. Miasik, A. Hooper, B. C. J. Tofield, Chem. Soc. Faraday Trans. I 1986, 82, 1117-
8
9 1126.
10
11 [18] X. Ma, G. Li, M. Wang, Y. Cheng, R. Bai, H. Chen, , Chem. Euro. J. 2006, 12, 3254-
12
13 3260.
14
15 [19] P. N. Bartlett, S. K. C. Liang, Sens. Actuators B 1989, 20, 287-292.
16
17 [20] H. Perez, J. P. Pradeau, P. A. Albouy, J. Perez-Omil, Chem. Mater. 1999, 11, 3460-
18
19 3463.
20
21
22
23
24
25
26
27
28
29
30
31
32
33
34
35
36
37
38
39
40
41
42
43
44
45
46
47
48
49
50
51
52
53
54
55
56
57
58
59
60

1
2
3
4
5
6
7
8
9
10
11 **Figure caption.**
12
13
14
15
16
17
18
19
20
21
22
23
24
25
26
27
28
29
30
31
32
33
34
35
36
37
38
39
40
41
42
43
44
45
46
47
48
49
50
51
52
53
54
55
56
57
58
59
60

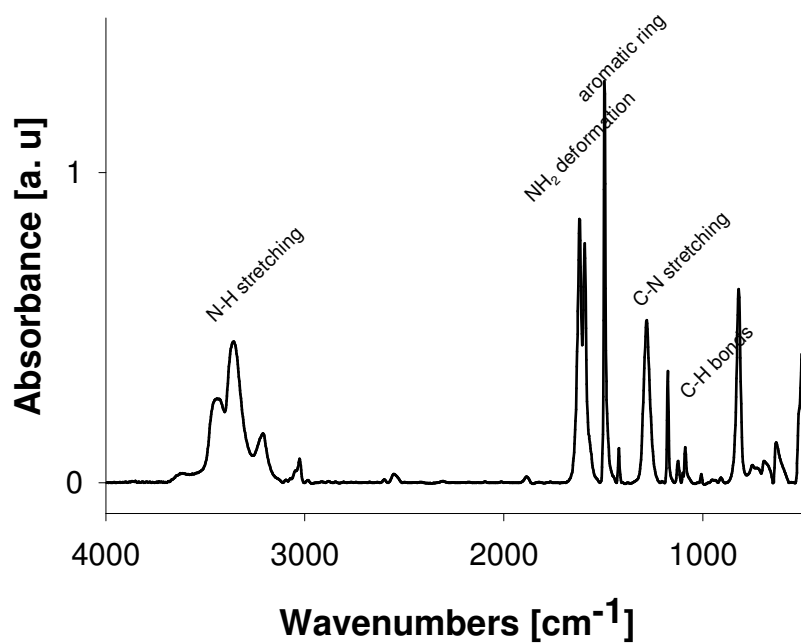


Figure 1. FTIR spectrum of functionalized Platinum nanoparticles with mercaptoaniline.

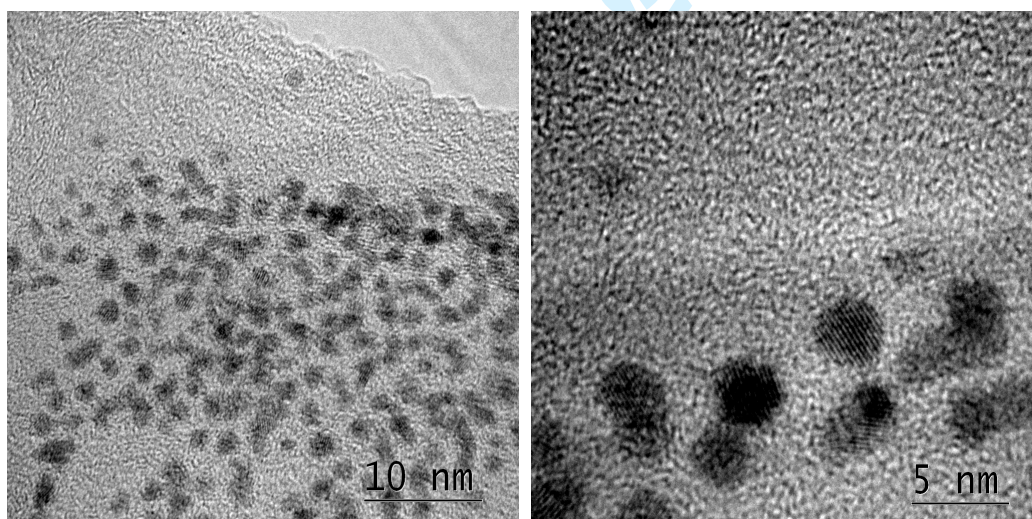


Figure 2. TEM pictures of functionalized Platinum nanoparticles with mercaptoaniline.

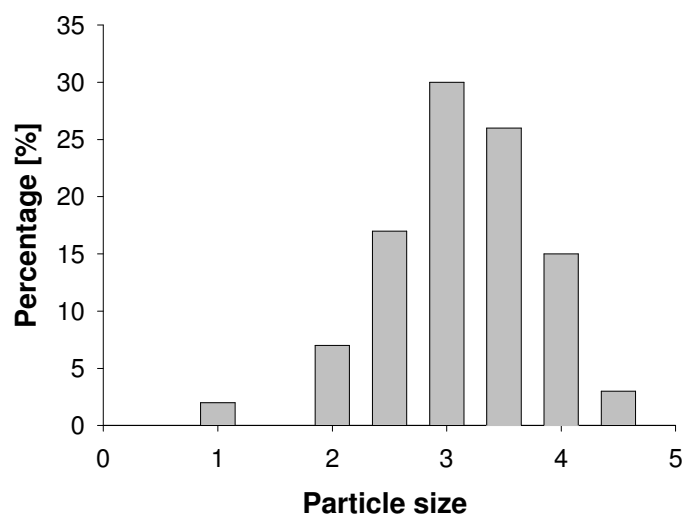


Figure 3. Histogram of functionalized Platinum nanoparticles diameters.

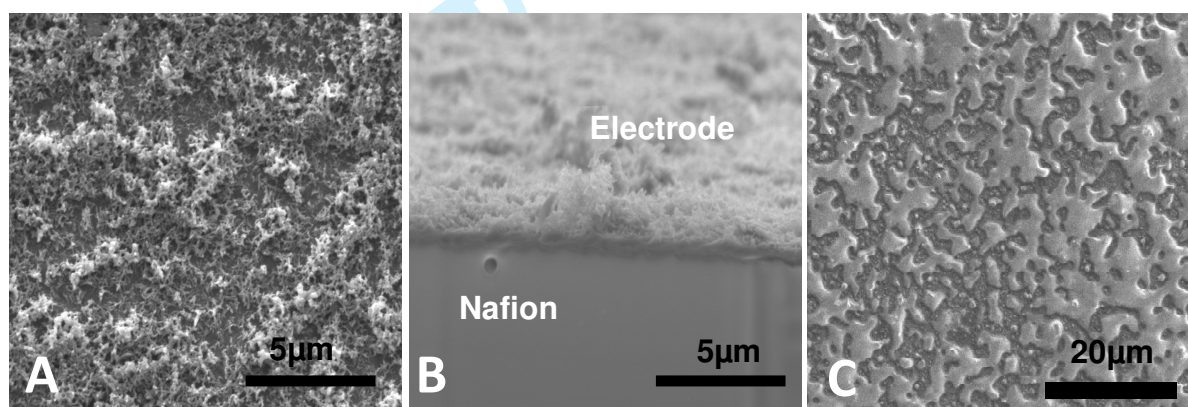


Figure 4. SEM picture of : A) Top-view of pPANI-Pt film coated onto a commercial Nafion 117 membrane; B) Cross-section of pPANI-Pt film coated onto a commercial Nafion 117 membrane; C) pPANI film obtained without Pt.

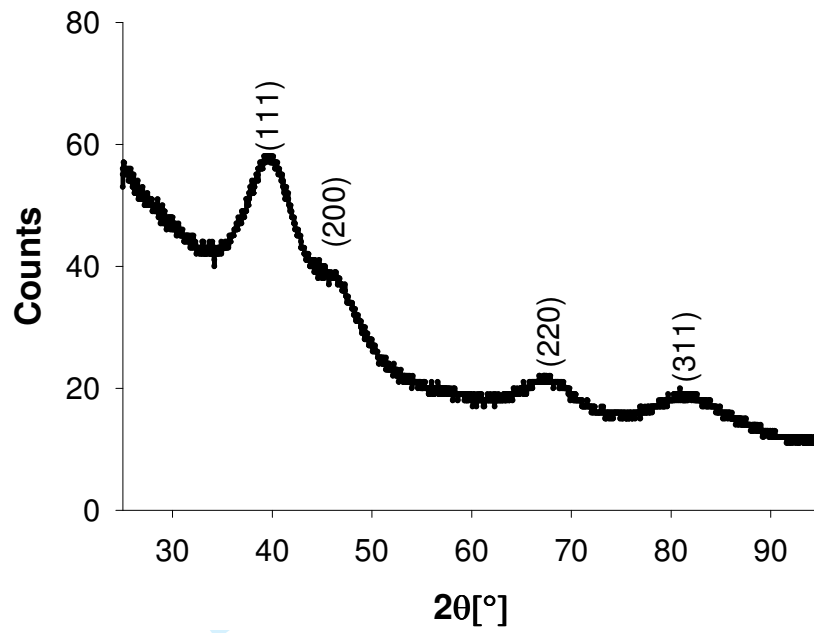


Figure 5. XRD pattern of pPANI-Pt coated onto a commercial Nafion 117 membrane.

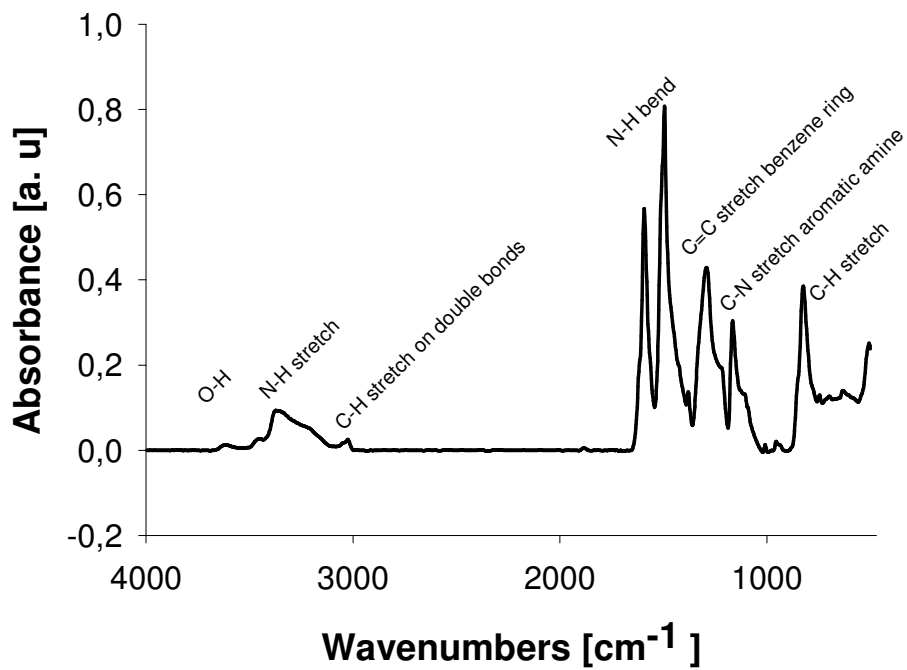


Figure 6. FTIR spectrum of the coated pPANI-Pt coated onto a Nafion 117 membrane.

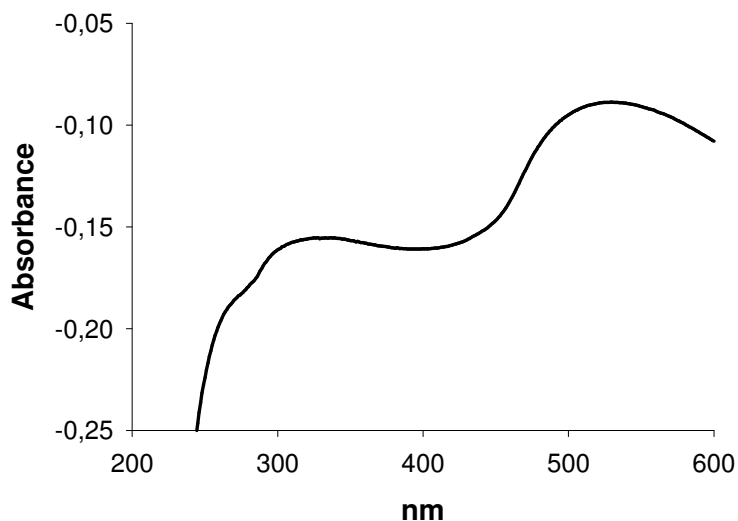


Figure 7. UV-Vis spectrum of pPANI-Pt film coated onto a commercial Nafion 117 membrane.

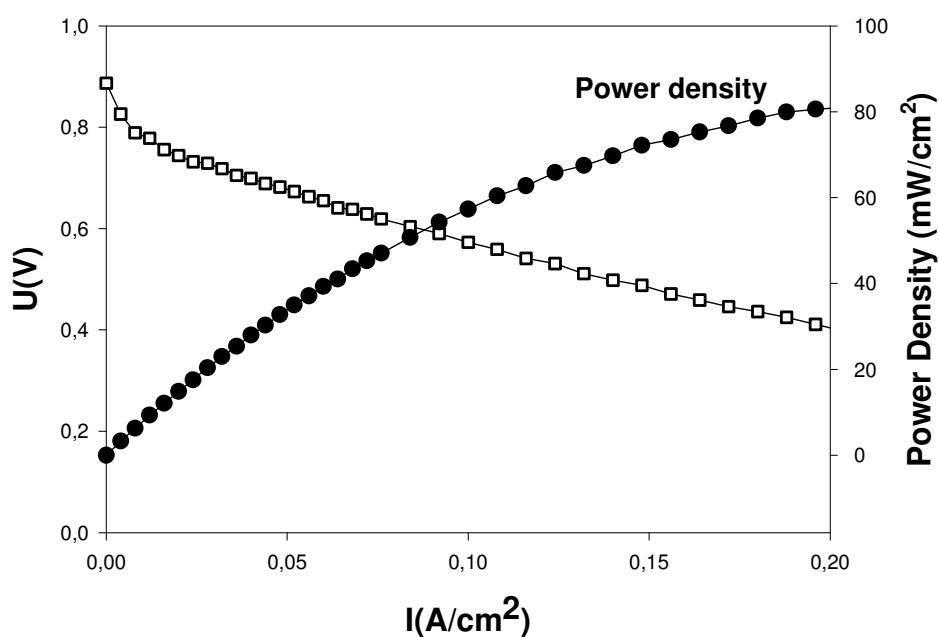
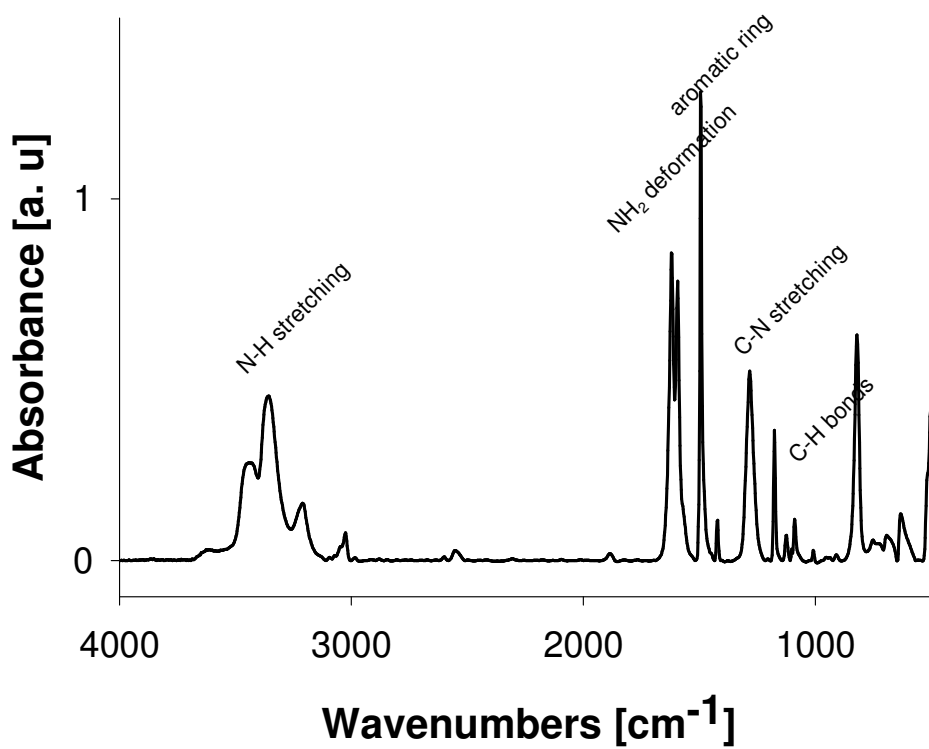


Figure 8. Polarization (\square) and power density curve (\bullet) of fuel cell. The fuel cell temperature was 80°C . H_2 and O_2 flows were set at $150 \text{ mL} \cdot \text{min}^{-1}$ and $75 \text{ mL} \cdot \text{min}^{-1}$, respectively.



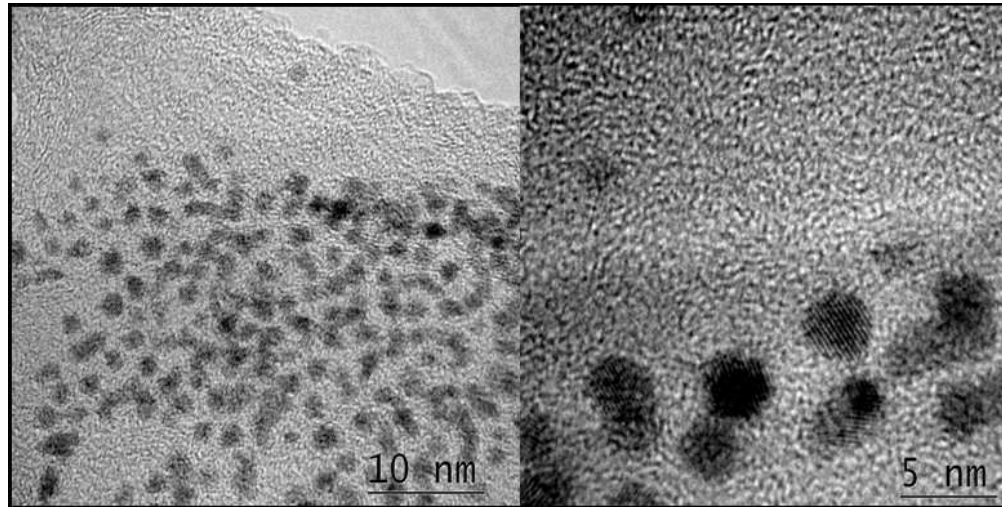
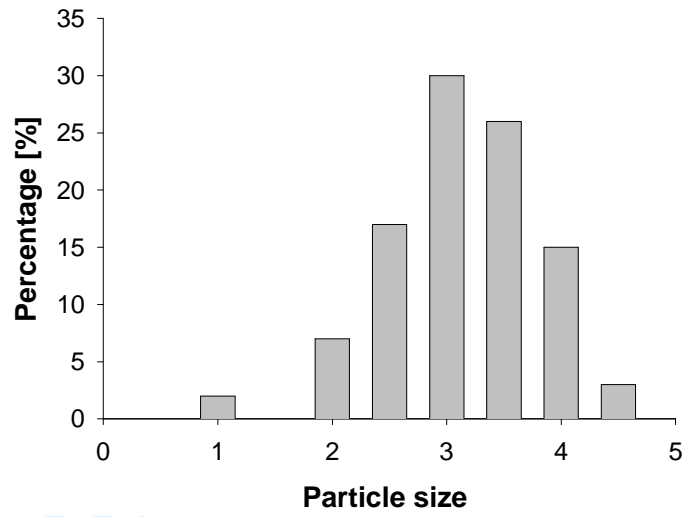


Figure 2. TEM pictures of functionalized Platinum nanoparticles with mercaptoaniline.
274x137mm (72 x 72 DPI)

Peer Review



For Peer Review

1
2
3
4
5
6
7
8
9
10
11
12
13
14
15
16
17
18
19
20
21
22
23
24
25
26
27
28
29
30
31
32
33
34
35
36
37
38
39
40
41
42
43
44
45
46
47
48
49
50
51
52
53
54
55
56
57
58
59
60

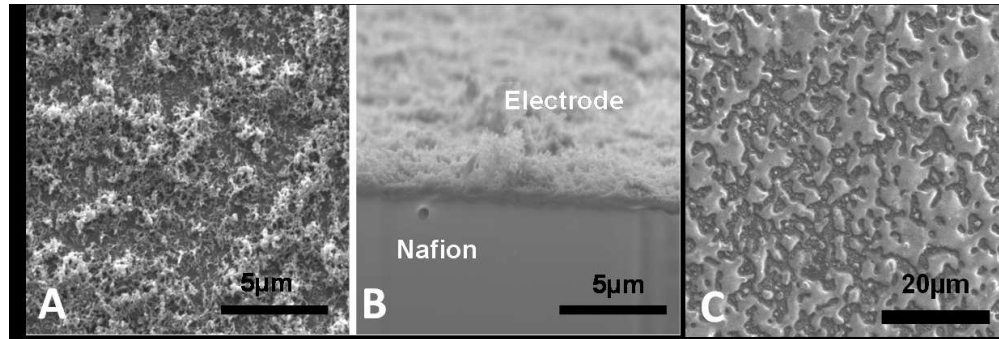
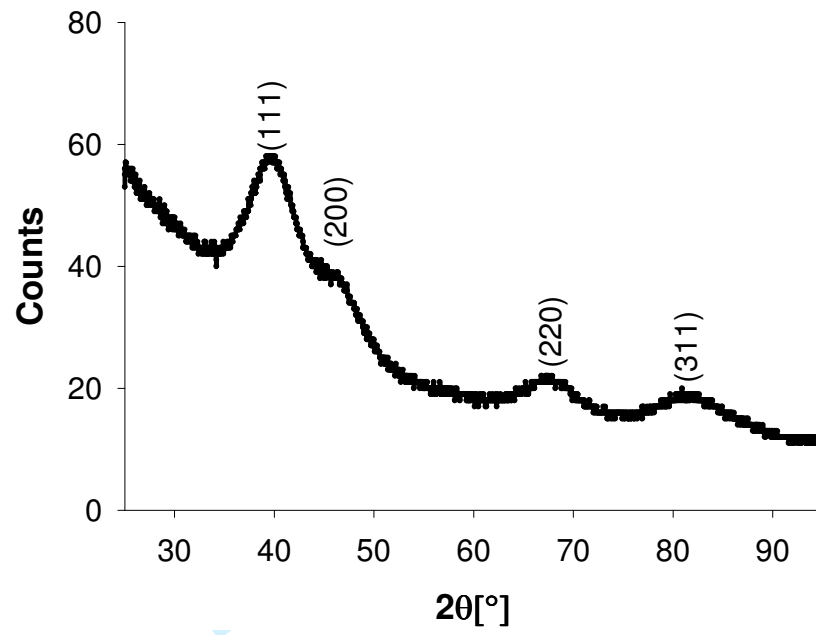
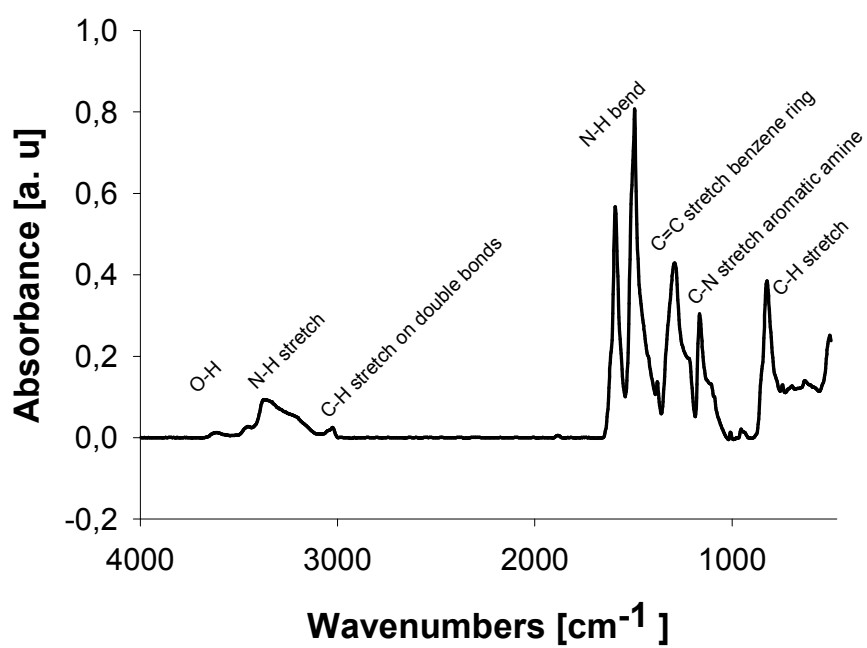


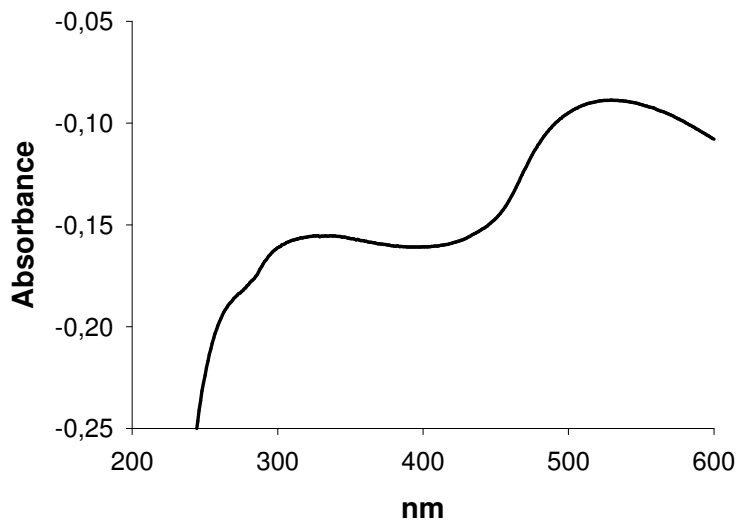
Figure 4. SEM picture of : A) Top-view of pPANI-Pt film coated onto a commercial Nafion 117 membrane; B) Cross-section of pPANI-Pt film coated onto a commercial Nafion 117 membrane; C) pPANI film obtained without Pt.
436x146mm (72 x 72 DPI)



Peer Review

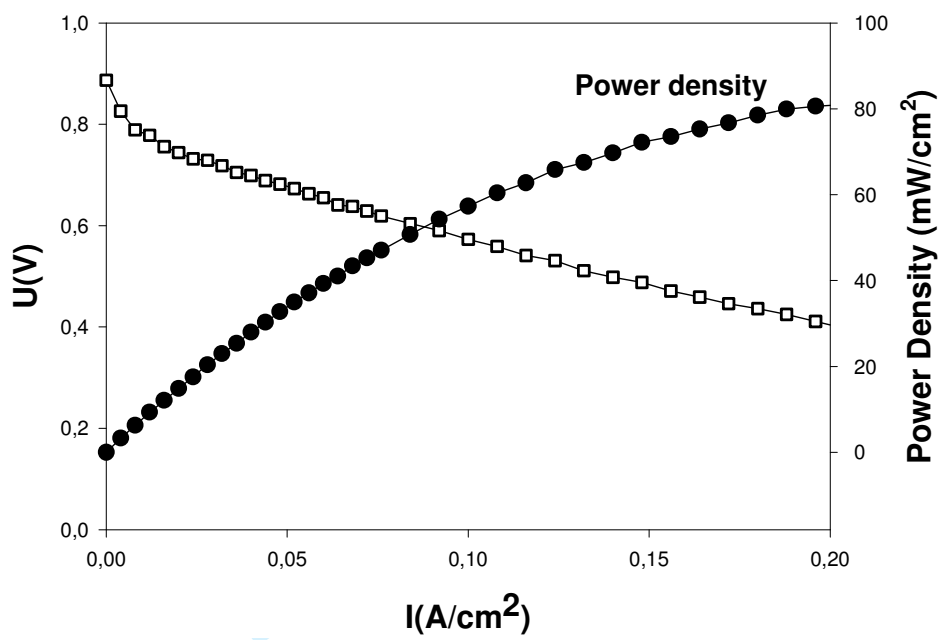


Peer Review



Or Peer Review

1
2
3
4
5
6
7
8
9
10
11
12
13
14
15
16
17
18
19
20
21
22
23
24
25
26
27
28
29
30
31
32
33
34
35
36
37
38
39
40
41
42
43
44
45
46
47
48
49
50
51
52
53
54
55
56
57
58
59
60



Peer Review

1
2
3
4
5
6
7
8
9
10
11
12
13
14
15
16
17
18
19
20
21
22
23
24
25
26
27
28
29
30
31
32
33
34
35
36
37
38
39
40
41
42
43
44
45
46
47
48
49
50
51
52
53
54
55
56
57
58
59
60